Adsorption of cadmium onto Al$_{13}$-pillared acid-activated montmorillonite

Liang-guo Yan [a], Xiao-quan Shan [a,*],
Bei Wen [a], Gary Owens [b]

[a] *State Key Laboratory of Environmental Chemistry and Ecotoxicology, Research Center for Eco-Environmental Sciences,*
Chinese Academy of Sciences, P.O. Box 2871, Beijing 100085, China
[b] *Centre for Environmental Risk Assessment and Remediation, University of South Australia, Mawson Lakes Campus,*
Mawson Lakes, Boulevard, South Australia 5095, Australia

Abstract

The optimal preparation conditions for Al$_{13}$-pillared acid-activated Na$^+$-montmorillonite (Al$_{13}$-PAAMt) were (1) an acid-activated Na$^+$-montmorillonite (Na$^+$-Mt) solution of pH 3.0, (2) a OH$^-$/Al^{3+} molar ratio of 2.4 and (3) Al^{3+}/Na$^+$-Mt ratio of 1.0 mmol g^{-1}. The effects of OH$^-$/Al^{3+} and Al^{3+}/Na$^+$-Mt ratios on the adsorption of Cd^{2+} onto Al$_{13}$-PAAMt were studied. A comparison of the adsorption of Cd^{2+} onto Al$_{13}$-PAAMt, Al$_{13}$-pillared Na$^+$-montmorillonite (Al$_{13}$-PMt) and Na$^+$-Mt suggested that Al$_{13}$-PAAMt had higher adsorption affinity for Cd^{2+} than the other two adsorbents. A pseudo-second-order model described the adsorption kinetics well. Cadmium adsorption followed the Langmuir two-site equation, while desorption was hysteretic.
© 2007 Elsevier B.V. All rights reserved.

Keywords: Al$_{13}$-pillared acid-activated montmorillonite; Al$_{13}$; Cd^{2+}; Adsorption kinetics; Hysteretic desorption

1. Introduction

The release of heavy metals into the environment is a potential threat to water and soil quality as well as to plant, animal and human health. Heavy metals can be bioaccumulated through food chain transfers and unlike organic toxicants are not amenable to biological degradation. Cadmium (Cd) is one toxic heavy metal of particular environmental concern, because it can be introduced into and accumulated in soils through agricultural application of sewage sludge, fertilizers, and/or through land disposal of Cd-contaminated municipal and industrial wastes. Cd is a known human carcinogen and may induce lung insufficiency, bone lesions and hypertension [1]. The high toxicity of cadmium has resulted in governments imposing ever tighter environmental legislation limiting wastewater discharge and the removal of heavy metals such as Cd from wastewater has been a major preoccupation of environmental professionals for many years. In particular, ever

increasing world populations are likely to place increasing stress on a limited clean water resource placing a greater focus on clean up and reuse of contaminated wastewater streams.

Of the various remediation techniques commonly available for the removal of heavy metals from aqueous solutions, adsorption onto a low-cost particulate media, such as a clay mineral, offers an attractive and inexpensive remediation option [2]. Clays are abundant, cheap, negatively charged layered aluminosilicate minerals that make good cationic adsorbents due to their relatively large surface areas. Clays adsorb heavy metals via ion exchange reactions and by the formation of inner-sphere complexes through ≡Si–O$^-$ and ≡Al–O$^-$ groups at the clay particle edges [3,4].

The adsorption properties of natural clay minerals can often be improved either by intercalation of organic, inorganic, or organometallic molecules in the interlamellar space, or by heat or acid treatments [5–8]. Of these modifications, metal oxide-pillared interlayered clays have been most extensively studied in recent years [8–11]. While pillared clays are commonly used as catalysts, they are also finding applications as novel adsorbents. The advantages of pillared clays include increased surface area

* Corresponding author. Tel.: +86 10 62923560; fax: +86 10 62923563.
E-mail address: xiaoquan@rcees.ac.cn (X.-q. Shan).

and pore volumes, which results in greater adsorption capacity and better flow properties when compared to the unpillared parent clays.

Recently, adsorption of a variety of heavy metals onto pillared clays has been reported [12–22]. Cu adsorption was increased by the presence of hydroxyaluminum polymeric components on Wyoming montmorillonite [12] and electron spin resonance data confirmed chemisorption of Cu onto the hydroxyaluminum polymeric components of the pillared clay as well as evidence for electrostatically bound Cu^{2+}. Bergaoui et al. [13,14] indicated that both Cu and Cd were adsorbed onto aluminum-pillared clay through a mechanism different from cation exchange.

The solution pH may play an important role in determining the mechanism of cadmium adsorption by clays. Keizer and Bruggenwart [15] indicated that Cd adsorption by hydroxyaluminum-montmorillonite at pH 5.0 was an electrostatic process, but at pH 7.0 observed significant specific adsorption. Another research has indicated that a substantial portion of Cd is adsorbed by the interlayer material through specific adsorption [16–18].

Pillared interlayered clays are typically prepared by replacement of interlayer cations with polycations and subsequent calcination to form nanooxide aggregates in the interlayer spaces. The properties of a specific clay can be modified and optimized to suit a specific application by using different pillaring agents and pillaring procedures. Consequently, many different pillared clays have been synthesized. As well as the pillaring agent, the synthetic conditions including concentration of metal ions, pH, degree of hydrolysis, aging time, temperature and metal/clay ratio can all affect the physiochemical properties of the produced pillared clays and thus influence the adsorption behavior of heavy metals.

Treatment of clay minerals with inorganic acids at high concentrations, referred to as "acid activation", is an alternative modification method and acid-activated clays are commonly used both as adsorbents [23–26] and catalysts [6]. These two types of clay modifications can be combined to produce pillared acid-activated clays and have the effect of enhancing the acidity of the acid-activated clays and increasing the stability of the pillared bidimensional network. Jones and coworkers [27–31] reported that pillared acid-activated montmorillonite exhibited enhanced catalytic activity and adsorptive capabilities for the removal of chlorophyll from edible oils compared to unmodified clays.

While extensive studies on the adsorption behavior of heavy metals onto Al_{13}-pillared Na^+-montmorillonite (Al_{13}-PMt) has been conducted, very little information is available on the use of Al_{13}-pillared acid-activated Na^+-montmorillonite (Al_{13}-PAAMt) as adsorbents for heavy metals. Therefore, the aim of this study was to optimize the synthetic conditions for Al_{13}-PAAMt to enhance the adsorbent properties of the clay for Cd^{2+} and to compare the adsorption behavior of Cd^{2+} on Al_{13}-PAAMt with that of conventionally produced on Al_{13}-PMt and Na^+-montmorillonite (Na^+-Mt).

2. Materials and methods

2.1. Montmorillonite

Unmodified montmorillonite was purchased from Beijing Youlichuangjia Science & Technology Development Company (Beijing, China). According to the supplier, the natural montmorillonite contained 98% montmorillonite, 0.5% kaolinite and 1.0% quartz. The chemical composition was SiO_2 (50.90%), Al_2O_3 (18.36%), Fe_2O_3 (1.03%), CaO (3.97%), MgO (4.14%), TiO_2 (0.02%), K_2O (0.72%), Na_2O (1.18%) and P_2O_5 (2.15%). Prior to use, montmorillonite was converted to Na^+-exchanged form by three ion-exchange reactions with $1.0\,mol\,L^{-1}$ NaCl and washed until free of chloride as indicated by the $AgNO_3$ test. The clay was dried at $80\,°C$ and ground to pass through a 100 mesh sieve. The treated Na^+-montmorillonite was designated Na^+-Mt.

2.2. Chemicals and solutions

All chemicals used in this work were of analytical grade reagents and were used without further purification. Water was double distilled from a MilliQ system and had a resistance <18 MΩ/cm.

A fresh aluminum-hydroxypolycation solution, $[Al_{13}O_4(OH)_{24}(H_2O)_{12}]^{7+}$, was prepared by drop-wise addition of NaOH ($0.2\,mol\,L^{-1}$) to $AlCl_3$ ($0.2\,mol\,L^{-1}$) solution with rapid mixing using a magnetic stirrer. Rapid agitation was necessary to prevent local over concentration of hydroxyl ions. The amounts of sodium hydroxide added were calculated to obtain OH^-/Al^{3+} molar ratios of 1.8, 2.0, 2.2 and 2.4. These solutions were subsequently aged for 5 days at room temperature prior to examination.

2.3. Preparation of pillared Na^+-montmorillonite

An aged Al_{13} stock solution ($[OH^-]/[Al^{3+}] = 2.4$) was slowly added to an aqueous slurry of Na^+-Mt (1% (w/w)) with continuous stirring. Since 1 g of montmorillonite adsorbs 2.0 mmol of Al^{3+} in the form of Al_{13}^{7+} addition continued until a ratio of Al^{3+}/Na^+-Mt equivalent to $2.0\,mmol\,g^{-1}$ clay was obtained. The pH of the mixture (pH 10.2) was unadjusted and the mixture was stirred for 24 h at room temperature. The resulting material was collected by centrifugation at 7000 rpm for 30 min and washed with double-distilled water until chloride-free as indicated by the $AgNO_3$ test. The product was dried at $80\,°C$ and gently ground in an agate mortar. This pillared Na^+-montmorillonite was designated Al_{13}-PMt.

2.4. Preparation of pillared acid-activated Na^+-montmorillonites

A montmorillonite slurry (1% (w/w)) was prepared by adding Na^+-Mt (1.0 g) to double-distilled water (100 mL) and stirred continually for 4 h. The pH of the slurry was then adjusted to 3.0 using $1.0\,mol\,L^{-1}$ HNO_3 and the mixture was stirred for a further 16 h at room temperature. During stirring, the pH was

Table 1
Basal spacing (d_{001}), BET surface area, total pore volume, average pore diameter and pH_{50} of Na^+-Mt, Al_{13}-PMt and Al_{13}-PAAMts

Adsorbent	Preparation conditions		d_{001} (Å)	BET surface area (m^2/g)	Total pore volume (mL/g)	Average pore diameter (Å)	pH_{50}
	OH^-/Al^{3+}	Al^{3+}/Na^+-Mt ($mmol\,g^{-1}$)					
Na^+-Mt	–	–	14.69	18.64	0.0343	73.59	7.08
Al_{13}-PMt	2.4	2.0	18.53	192.5	0.1162	18.27	6.58
Al_{13}-PAAMt	1.8	2.0	18.22	176.4	0.1090	18.64	6.03
	2.0	2.0	18.29	187.6	0.1139	18.34	5.92
	2.2	2.0	18.48	189.7	0.1122	17.90	5.94
	2.4	2.0	18.86	196.4	0.1220	18.76	5.95
Al_{13}-PAAMt	2.4	1.0	16.42	132.7	0.0876	19.86	5.38
	2.4	2.0	18.86	196.4	0.1220	18.76	5.96
	2.4	5.0	18.79	205.3	0.1271	18.70	6.08
	2.4	10.0	17.94	196.4	0.1212	18.65	6.18

measured every 6 h and readjusted to pH 3.0 as required with $1.0\,mol\,L^{-1}$ HNO_3.

In the first series of experiments, Al_{13}-PAAMts were prepared by the slow addition of Al_{13} solutions ($[OH^-]/[Al^{3+}]$ = 1.8, 2.0, 2.2 and 2.4) to a 1% (w/w) suspension of acid-activated Na^+-Mt with continual stirring to obtain a final ratio of Al^{3+}/Na^+-Mt equal to 2.0 $mmol\,g^{-1}$. Following final addition of the Al_{13} solutions the mixtures were stirred for 24 h, and the clay adsorbent separated from the solution by centrifugation at 7000 rpm for 30 min, washed with double-distilled water, dried at 80 °C and ground to a fine powder in an agate mortar and pestle prior to further analysis.

In the second series of experiments the Al^{3+}/Na^+-Mt ratio was varied from 1.0 to 10.0 $mmol\,g^{-1}$ montmorillonite. The pillaring procedure was the same as described above using a pillaring solution with $[OH^-]/[Al^{3+}]$ = 2.4.

2.5. Clay characterization

The d_{001} values (basal spacings) were recorded using $CuK\alpha$ radiation from an automated X-ray diffractometer (XRD) (Rigaku Geigerflex RAD3-C, Tokyo, Japan) equipped with a graphite monochromator. Montmorillonite samples were coated with Au under vacuum in an argon atmosphere for scanning electron microscopy (SEM) studies (Hitachi S570, Tokyo, Japan).

Surface area and pore size distributions were measured using nitrogen as sorbate at 77 K in a static volumetric apparatus (Micromeritics ASAP 2000, Micromeritics, USA). The samples were previously degassed at 120 °C for 16 h under vacuum. Specific surface areas were calculated by the Brunauer–Emmet–Teller (BET) equation. Pore size distributions were calculated using the Barrett–Joyner–Halenda (BJH) method.

2.6. Cd^{2+} adsorption

Cadmium adsorption experiments were conducted in triplicate at room temperature using a batch equilibration method. Adsorbent, Na^+-Mt or pillared montmorillonites

(0.100 g), was mixed with various concentrations of Cd^{2+} in $0.01\,mol\,L^{-1}$ $NaNO_3$ background electrolyte solution (20 mL) in 50 mL polypropylene centrifuge tubes. The pH of Cd^{2+}-montmorillonite suspension was adjusted to 6.5 by addition of either $0.1\,mol\,L^{-1}$ HNO_3 or $0.1\,mol\,L^{-1}$ NaOH. The pH was measured at 6 h intervals and readjusted to 6.5 as necessary. The suspension was shaken continuously for 24 h to ensure complete Cd^{2+} adsorption. Preliminary experiments (data not shown) indicated that adsorption was complete within 24 h. After centrifuging at 7000 rpm for 30 min the suspension was filtered through a 0.45 μm cellulose acetate membrane and the concentrations of Cd^{2+} in the filtrates were determined using inductively coupled plasma-atomic emission spectrometry (ICP-AES, OPTIMA2000DV, PerkinElmer, USA). The adsorbed Cd^{2+} was calculated from the differences between the initial and final equilibrium concentrations.

2.7. Cd^{2+} desorption

Desorption experiments were performed using sequential decant–refill steps immediately following the completion of the adsorption experiments. At the end of adsorption experiments, solids were separated from the aqueous solution by centrifugation and 10 mL of the supernatant solution was withdrawn for Cd^{2+} analysis. The remaining slurry was again brought to 20 mL by the addition of 10 mL of background desorption solution ($0.01\,mol\,L^{-1}$ $NaNO_3$ solution adjusted to pH 6.5), and then the suspension was shaken for an additional 24 h. These steps were repeated three more times and the concentration of Cd^{2+} in the supernatant after each desorption cycle was determined. The amount of Cd^{2+} remaining in the adsorbent after each desorption step was calculated as the difference between the amount of Cd^{2+} initially adsorbed and the final amount of Cd^{2+} desorbed.

2.8. Cd^{2+} adsorption kinetics and pH effects

Experiments examining the adsorption kinetics and the effect of pH on Cd^{2+} adsorption were also conducted. The initial Cd^{2+} concentration was $0.1\,mmol\,L^{-1}$. The pH of the Cd^{2+}-
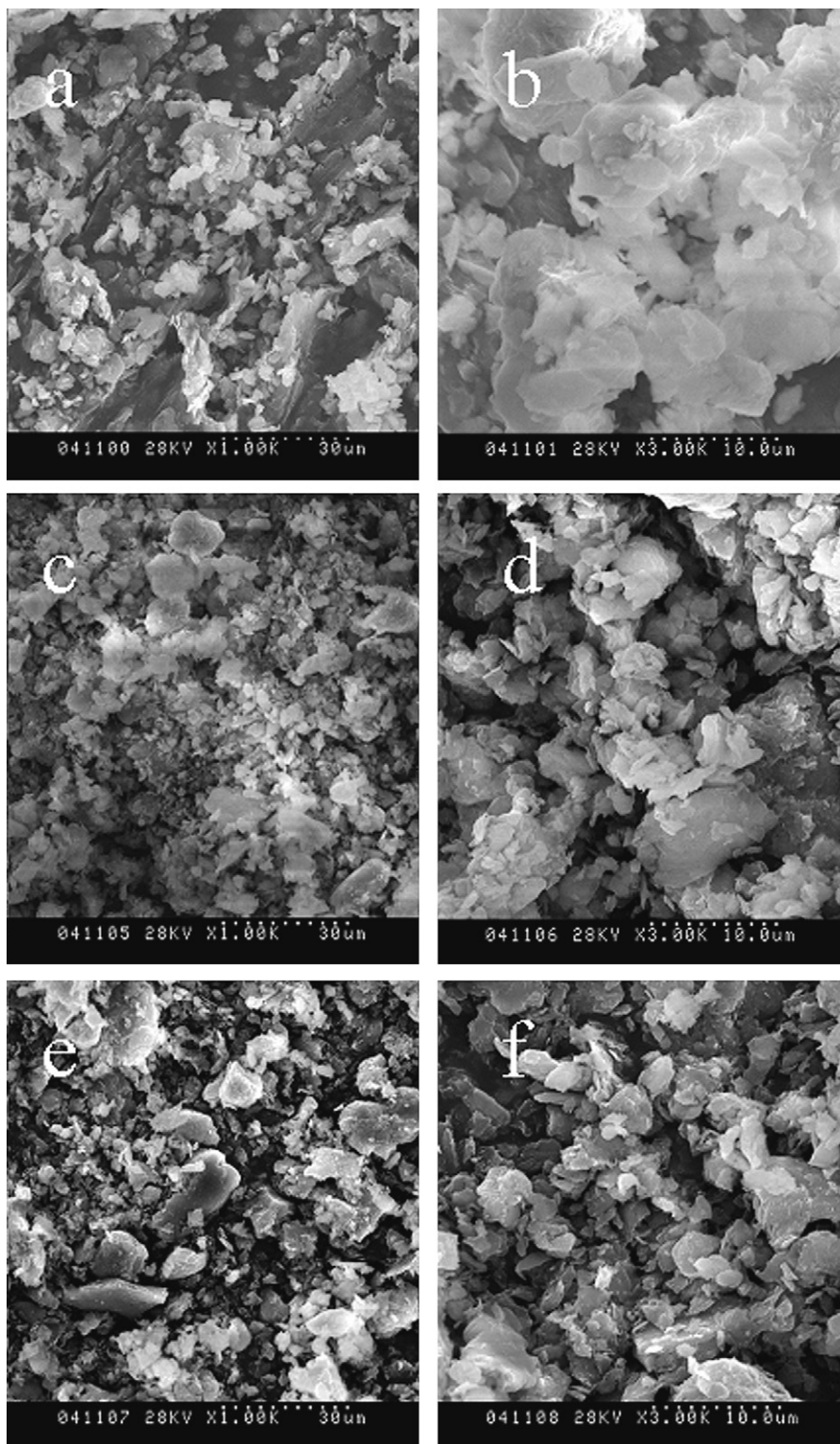
Fig. 1. SEM images of Na$^+$-Mt (a, b), Al$_{13}$-PMt (c, d) and Al$_{13}$-PAAMt (e, f) at different magnifications (10 μm and 30 μm).

montmorillonite was maintained at 6.5 throughout the kinetics experiments.

Experiments examining the pH effect on Cd^{2+} adsorption involved a two-step pH adjustment. Suspensions of adsorbent, Na$^+$-Mt, Al$_{13}$-PMt or Al$_{13}$-PAAMt, (0.100 g) were initially sus-pended in 0.01 mol L^{-1} NaNO$_3$ (19 mL) and the pH adjusted to approximately 4–9. Subsequently, 2.0 mmol L^{-1} Cd^{2+} as the nitrate salt (1.0 mL) was added. The suspensions were shaken for 24 h and another pH adjustment was conducted at 6 h inter-vals.

3. Results and discussion

3.1. Characterization of the pillared Na+-montmorillonites

Three main variables controlling the quality of pillared clays included suspension pH, the OH^-/Al^{3+} molar ratio and the Al^{3+}/Na^+-Mt ratio. The initial pH of Na^+-Mt suspension was either acid activated to pH 3.0 or unadjusted (pH 10.2), the OH^-/Al^{3+} molar ratio varied from 1.8 to 2.4 and the Al^{3+}/Na^+-Mt ratio varied from 1.0 to 10.0 mmol g^{-1}.

Prepared montmorillonites were characterized in terms of basal spacing, specific surface area and porosity (Table 1). X-ray diffractograms of the Na^+-Mt showed an intense d_{001} peak at 6.04°, corresponding to a basal spacing of 14.69 Å. The BET surface area was 18.64 m^2/g. After pillaring with Al_{13}, the basal spacing and surface area were increased to 18 Å and 200 m^2/g, respectively. The pillared montmorillonites had similar basal spacings, indicating that the composition of the Al_{13} pillaring solution did not cause significant changes in the final basal spacing.

Addition of Al_{13} pillaring solutions with increasing OH^-/Al^{3+} molar ratios resulted in a slight increase in the surface area and total pore volume of Al_{13}-PAAMt. Al_{13}-PAAMts synthesized with 2.0, 5.0, and 10.0 mmol g^{-1} acid-activated Na^+-Mt had similar surface areas and porosity but specific surface area and total pore volume of the Al_{13}-PAAMts were approximately 10- and 3-fold larger, respectively, than those of unpillared Na^+-Mt. Meanwhile, the average pore diameter decreased from 73.59 to 20 Å. These results suggested that the pillaring process generated micropores, indicating intercalation of inorganic polyoxycations between the clay layers.

SEM was used to study the changes in morphology of Na^+-Mt, Al_{13}-PMt and Al_{13}-PAAMt (Fig. 1). Na^+-Mt exhibits a lamellar structure (Fig. 1a) and an aggregated morphology (Fig. 1b) and some large flakes were observed in some instances. After modification with Al_{13}, a number of lamellas arranged to form a stacking structure (Fig. 1c–f) making the intraparticle voids smaller, which was consistent with the larger BET surface area when compared to the unpillared Na^+-Mt. The Al_{13}-PAAMt had more compacted structure than Al_{13}-PMt.

3.2. Effects of preparative conditions on Cd2+ adsorption onto Al13-PAAMt

The dependence of Cd^{2+} adsorption on preparation conditions including (1) initial pH of Na^+-Mt, (2) the OH^-/Al^{3+} molar ratio (data not shown) and (3) the Al^{3+}/Na^+-Mt ratio on Cd^{2+} adsorption is shown in Fig. 2. All pillared montmorillonites had a high adsorption affinity for Cd^{2+}, and all the adsorption isotherms of Cd^{2+} display a typical adsorption edge. The adsorption of Cd^{2+} begins below pH 5.0, then increases dramatically and essentially 100% adsorption is observed above pH 8.0. Similar pH dependence of Cd^{2+} adsorption has been reported in literature [17,18].

The pH value, at which 50% of the initial heavy metal ions were adsorbed, identified in Fig. 2 as a dashed line, was
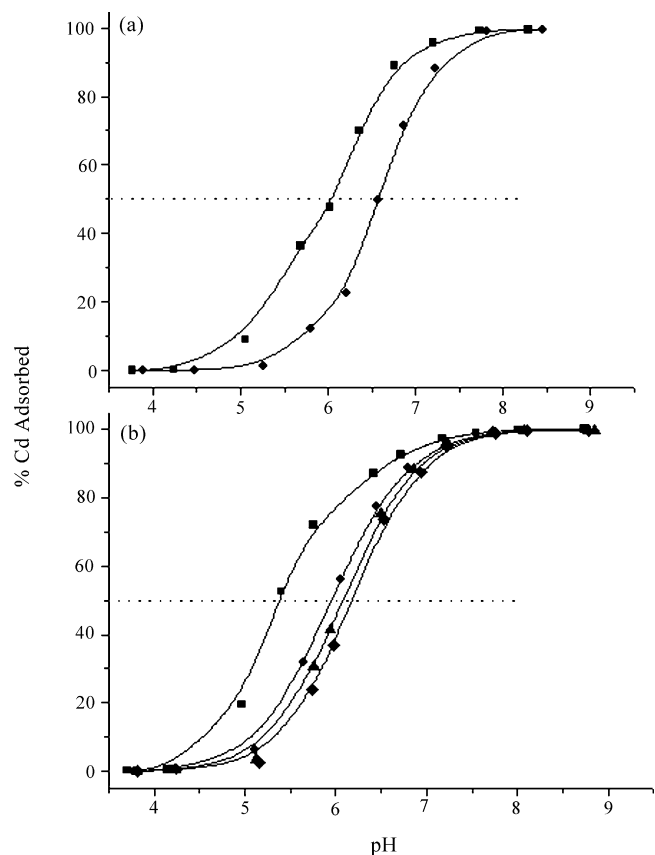

Fig. 2. Adsorption of 0.1 mmol L^{-1} Cd^{2+} as a function of pH by (a) Al_{13}-PAAMt (■) and Al_{13}-PMt (●) (preparation conditions: $[OH^-]/[Al^{3+}] = 2.4$ and Al^{3+}/Na^+-Mt ratio = 2.0 mmol g^{-1}) and (b) Al_{13}-PAAMts (preparation conditions: $[OH^-]/[Al^{3+}] = 2.4$ and Al^{3+}/Na^+-Mt ratio = 1.0 mmol g^{-1} (■), 2.0 mmol g^{-1} (●), 5.0 mmol g^{-1} (▲) and 10.0 mmol g^{-1} (♦)).

termed pH_{50}. pH_{50} is a measure of the selectivity of metal cations for the adsorbent surface [17,32]. The smaller the pH_{50}, the higher the selectivity of metal cations for adsorbent surface. The pH_{50} values of different pillared montmorillonites are summarized in Table 1. As shown in Fig. 2 and Table 1, Al_{13}-PAAMt showed a clearly higher affinity for Cd^{2+} than Al_{13}-PMt. While for Al_{13}-PAAMts, the effect of OH^-/Al^{3+} molar ratio on Cd^{2+} adsorption was almost insignificant (data not shown), the Al^{3+}/Na^+-Mt ratio had a pronounced effect on the Cd^{2+} adsorption. The adsorption of Cd^{2+} increased as the Al^{3+}/Na^+-Mt ratio of Al_{13}-PAAMt decreased from 10.0 to 1.0 mmol g^{-1}. The optimized conditions for preparation of Al_{13}-PAAMt were, therefore, pH 3.0 for acid-activated Na^+-Mt, with $[OH^-]/[Al^{3+}] = 2.4$ and an Al^{3+}/Na^+-Mt ratio of 1.0 mmol g^{-1}.

3.3. A comparative study of Cd2+ adsorption onto Al13-PAAMt, Al13-PMt and Na+-Mt

The synthetic conditions that resulted in optimal Cd^{2+} adsorption were used to prepare Al_{13}-PAAMt and a comparison was made between the adsorption behavior of Cd^{2+} on Al_{13}-PAAMt with that of Al_{13}-PMt and Na^+-Mt.
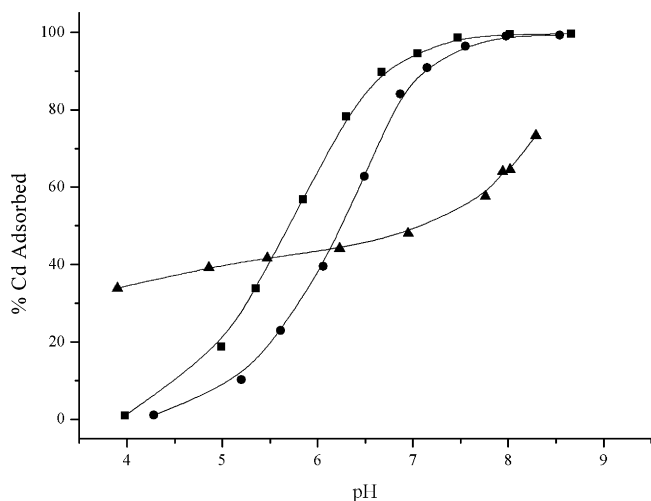
Fig. 3. Adsorption of 0.1 mmol L^{-1} Cd^{2+} as a function of pH by Al$_{13}$-PAAMt (■), Al$_{13}$-PMt (●) and Na$^+$-Mt (▲); [OH$^-$]/[Al^{3+}] = 2.4 and Al^{3+}/Na$^+$-Mt ratio = 1.0 mmol g^{-1}.

3.3.1. Effect of pH

Al$_{13}$-PAAMt and Al$_{13}$-PMt showed very different Cd^{2+} adsorption behavior than Na$^+$-Mt (Fig. 3). At low pH (up to 5.5 on Al$_{13}$-PAAMt and 6.1 on Al$_{13}$-PMt), Na$^+$-Mt adsorbed larger amounts of Cd^{2+} than either Al$_{13}$-PAAMt or Al$_{13}$-PMt. As the pH rose, Cd^{2+} adsorption onto Al$_{13}$-PAAMt and Al$_{13}$-PMt steeply increased and plateaued above pH 8 where adsorption was almost 100%. Adsorption of Cd^{2+} onto Al$_{13}$-PAAMt and Al$_{13}$-PMt showed a much stronger pH dependence when compared to that of Na$^+$-Mt. A clear adsorption edge can be detected for the adsorption of Cd^{2+} on both Al$_{13}$-PAAMt and Al$_{13}$-PMt. The adsorption edge for Al$_{13}$-PMt, however, shifted slightly towards higher pH. Na$^+$-Mt showed a less dramatic variation in Cd^{2+} adsorption with increasing pH and showed little evidence for an adsorption edge.

The effect of pH may be interpreted on the basis of availability of binding sites present at the clay surface. For Na$^+$-Mt, Cd^{2+} adsorption from solution can be described by utilization of both ion exchange sites and specific adsorption sites. At low pH, Cd is predominantly adsorbed on the permanent charge sites of Na$^+$-Mt. However, a substantial portion of Cd^{2+} was probably adsorbed on the edge surfaces at higher pH [17,18,33]. After treatment with Al$_{13}$, the cation exchange capacity of Na$^+$-Mt was reduced [18] and the low-affinity sites on the permanently charged Na$^+$-Mt surface are replaced by high-affinity aluminum hydroxyl functional groups with variable charge. This explains the observation that adsorbed Cd^{2+} increases at high pH with Al$_{13}$-PAAMt and Al$_{13}$-PMt due to increases in variable charge while Na$^+$-Mt shows no dramatic change in Cd^{2+} adsorption with increasing pH due to a permanent surface charge.

3.3.2. Adsorption kinetics

The adsorption kinetics of the three clay adsorbents are summarized in Fig. 4. When compared to Na$^+$-Mt pillaring of montmorillonite by Al$_{13}$ enhanced Cd^{2+} adsorption and altered the rate of adsorption. Unlike Na$^+$-Mt, sharp increase in the adsorption of Cd^{2+} was observed on the pillared montmorillonite
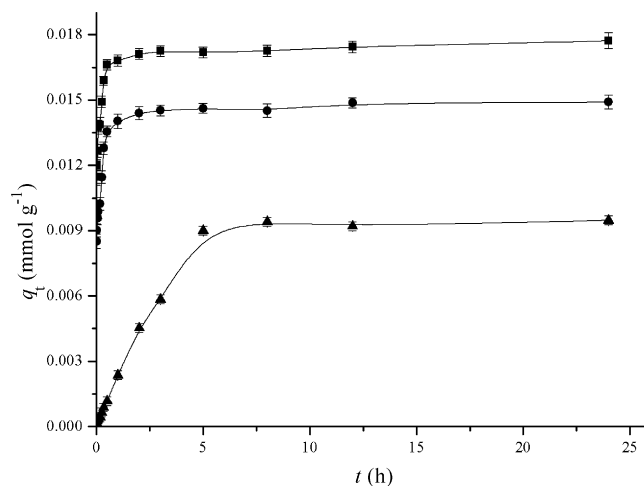

Fig. 4. Adsorption kinetics of Cd^{2+} for Al$_{13}$-PAAMt (■), Al$_{13}$-PMt (●) and Na$^+$-Mt (▲).

within the first hour and equilibrium conditions were obtained only after 2 h for Al$_{13}$-PAAMt and Al$_{13}$-PMt compared to 5 h for Na$^+$-Mt.

To evaluate the differences in adsorption kinetics between adsorbents, Cd^{2+} adsorption was analyzed using a pseudo-first- and pseudo-second-order model. Only the pseudo-second-order equation is applicable which is expressed by [34]:

$$\frac{dq_t}{dt} = k(q_e - q_t)^2 \qquad (1)$$

where q_e (mmol g^{-1}) and q_t (mmol g^{-1}) are the amount of solute adsorbed by adsorbent at equilibrium and at time t (h), respectively and k is the rate constant (g mmol^{-1} h^{-1}).

Integrating and rearranging Eq. (1) for the boundary conditions $t = 0$ to $t = t$ and $q_t = 0$ to $q_t = q_t$, allows a linear form to be derived.

$$\frac{t}{q_t} = \frac{1}{kq_e^2} + \frac{1}{q_e}t \qquad (2)$$

Thus, a plot of t/q_t against t should give a linear relationship with a slope of $1/q_e$ and an intercept of $1/kq_e^2$. The constants k and q_e (Table 2) were calculated from a linear regression plot of t/q_t versus t.

The kinetic data fit the pseudo-second-order model with correlation coefficients higher than 0.98 indicating that the kinetic model was appropriate. Similar studies have also been previously reported [19,35]. As can be seen from Table 2, the k_2 values of Cd^{2+} adsorption on Al$_{13}$-PAAMt and Al$_{13}$-PMt (1085 and 1008 g mmol^{-1} h^{-1}) were significantly greater than that of Na$^+$-Mt (36.86 g mmol^{-1} h^{-1}).

Table 2
Pseudo-second-order kinetic parameters for the adsorption of Cd^{2+} on Na$^+$-Mt, Al$_{13}$-PMt and Al$_{13}$-PAAMt

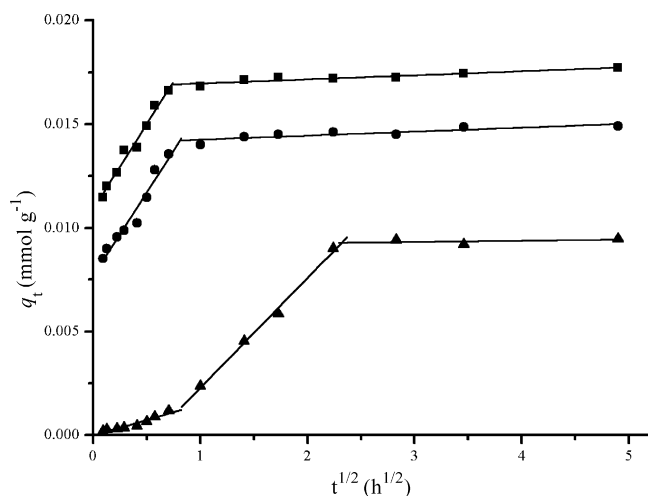| Adsorbent	k (g mmol^{-1} h^{-1})	q_e (mmol g^{-1})	R^2
Na$^+$-Mt	36.86	0.0108	0.9819
Al$_{13}$-PMt	1085	0.0149	0.9999
Al$_{13}$-PAAMt	1008	0.0177	0.9999

Fig. 5. Intraparticle diffusion model fit of Cd^{2+} adsorption on Al_{13}-PAAMt (■), Al_{13}-PMt (●) and Na^+-Mt (▲).

Fig. 6. Adsorption isotherms of Cd^{2+} to Al_{13}-PAAMt (■), Al_{13}-PMt (●) and Na^+-Mt (▲).

To better understand the adsorption mechanism, the experimental data was also tested using an intraparticle diffusion model as expressed by Weber and Morris [36]:

$$q_t = k_d t^{1/2} \tag{3}$$

where q_t (mmol g^{-1}) is the amount of Cd^{2+} adsorbed at time t (h) and k_d is the intraparticle diffusion rate constant (mmol g^{-1} h$^{-1/2}$). According to this model, several mechanisms are involved and the adsorption process can be characterized into three steps: (1) external surface adsorption, (2) intraparticle diffusion which is the rate-limiting step, and (3) the final equilibrium which is very fast [37].

A plot of q_t versus $t^{1/2}$, as shown in Fig. 5, represents three different stages of Cd^{2+} adsorption. For Al_{13}-PMt and Al_{13}-PAAMt, the adsorption processes of Cd^{2+} are comprised of two phases, suggesting that intraparticle diffusion is not a rate-limiting step for this material [36]. The initial portion of plot indicated an external mass transfer and intraparticle or pore diffusion whereas the second linear portion was due to the final equilibrium. In comparison, for Na^+-Mt, three distinct steps were observed. The first step was diffusion of Cd^{2+} to the external surface, or boundary layer of the solute molecule, the
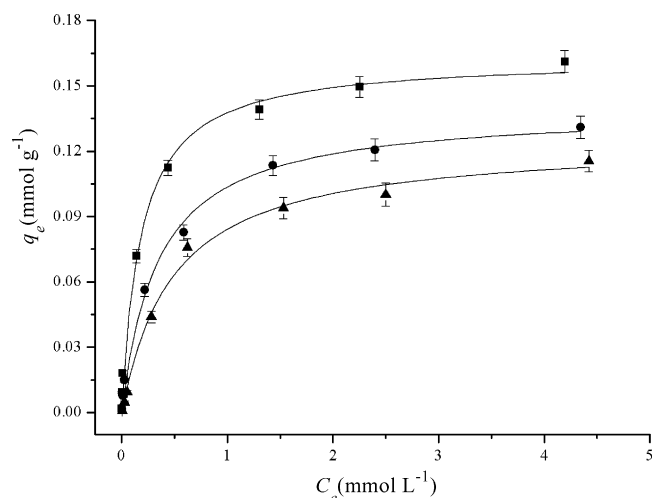
second step was intraparticle diffusion, which was a rate-limiting process and the third step was the final equilibrium stage for which the intraparticle diffusion started to slow down due to the extremely low Cd^{2+} concentration remaining in solution. Similar results have been reported for the adsorption of Co^{2+} by Al-pillared bentonite [38], Ni^{2+} by Na-mordenite [39] and other metal ions (Cd^{2+}, Cu^{2+}, Co^{2+}, Ni^{2+}, Pb^{2+}, Zn^{2+}) by untreated low-rank coal (oxihumolite) [40].

3.3.3. Adsorption isotherms

Fig. 6 compares adsorption isotherms of Cd^{2+} on Al_{13}-PAAMt and Al_{13}-PMt with that of unpillared Na^+-Mt. Langmuir one-site, Langmuir two-site and Freundlich equations [32] were used to model adsorption data.

$$q_e = \frac{bq_m C_e}{1 + bC_e} \tag{4}$$

$$q_e = \frac{b_1 q_{m,1} C_e}{1 + b_1 C_e} + \frac{b_2 q_{m,2} C_e}{1 + b_2 C_e} \tag{5}$$

$$q_e = K_f C_e^{1/n} \tag{6}$$

Table 3
Freundlich and Langmuir constants and correlation coefficients for the adsorption of Cd^{2+} on Na^+-Mt, Al_{13}-PMt and Al_{13}-PAAMt

Model	Parameter	Al_{13}-PAAMt	Al_{13}-PMt	Na^+-Mt
Freundlich equation	K_f	0.1183	0.0882	0.0706
	n	0.2790	0.3347	0.3874
	R^2	0.9596	0.9599	0.9408
Langmuir one-site equation	q_m (mmol kg^{-1})	0.1628	0.1393	0.1249
	b (L mmol^{-1})	5.483	2.899	2.582
	R^2	0.9936	0.9962	0.9949
Langmuir two-site equation	$q_{m,1}$ (mmol kg^{-1})	0.1332	0.1151	0.6244
	b_1 (L mmol^{-1})	3.033	1.654	4.546
	$q_{m,2}$ (mmol kg^{-1})	0.0353	0.0306	0.7456
	b_2 (L mmol^{-1})	79.05	19.76	4.493
	q'_m (mmol kg^{-1})	0.1685	0.1457	0.1370
	R^2	0.9994	0.9992	0.9961

where C_e (mmol L^{-1}) and q_e (mmol g^{-1}) are Cd^{2+} equilibrium concentrations in the aqueous and solid phases, respectively; q_m (mmol g^{-1}) is maximum adsorption capacity; $q_{m,1}$ and $q_{m,2}$ are maximum numbers of adsorption sites for two different sites, respectively; b, b_1, and b_2 are adsorption equilibrium constants; K_f is the equilibrium constant indicative of adsorption capacity and $1/n$ is an adsorption constant, whose reciprocal is indicative of adsorption intensity. For the Langmuir two-site model fit, the total adsorption maximum capacity, q'_m should be as follows:

$$q'_m = q_{m,1} + q_{m,2} \tag{7}$$

The adsorption parameters from the three models are summarized in Table 3. All models fit the adsorption data fairly well. The best numerical fit of the data was obtained using the more complex Langmuir two-site model. The fit of experimental data to the simpler Freundlich model was poorer than either the Langmuir one-site or Langmuir two-site models, in agreement with Matthes et al. [41]. The Langmuir two-site model was developed on the basis of Langmuir one-site model to solve the heterogeneity problem of adsorption sites. It has been successfully applied to represent equilibrium adsorption data of Cd^{2+} onto bone char [42], Pb^{2+} onto activated carbon [43] and heavy metals on peat [32].

From Table 3, the adsorption capacities of Cd^{2+} (q'_m) followed the order of Al$_{13}$-PAAMt > Al$_{13}$-PMt > Na$^+$-Mt. The equilibrium constant b_2 value was much higher than b_1 for Al$_{13}$-PAAMt and Al$_{13}$-PMt (Table 3), indicating that the surface was heterogeneous. The high-energy sites with high equilibrium constant (b_2) had a significantly higher affinity than low-energy sites with a low equilibrium constant (b_1). High-energy sites on which Cd^{2+} was tightly held had a low adsorption maximum ($q_{m,2}$) and low-energy sites on which Cd^{2+} were loosely held had high adsorption maximum ($q_{m,1}$). The adsorption equilibrium constant (b_2) of Al$_{13}$-PAAMt was higher than those of either Al$_{13}$-PMt or Na$^+$-Mt (Table 3). Therefore, Al$_{13}$-PAAMt not only had a higher overall adsorption capacity, but also contained sites with higher binding energy for Cd^{2+}.

3.3.4. Desorption isotherms

Desorption experiments were performed to better understand the adsorption process. Desorption experiments are also of great practical importance in wastewater treatment applications because they give insight into the long-term stability of the adsorbed metal. Fig. 7 displays desorption isotherms of Cd^{2+} from the three adsorbents. Desorption isotherms exhibited hysteresis. The quantity of Cd^{2+} desorbed from the adsorbents after three cycles of desorption varied between 6.7% and 23.8% for Al$_{13}$-PAAMt, 8.2% and 15.1% for Al$_{13}$-PMt, and 13.4% and 17.8% for Na$^+$-Mt, depending on the initial load of Cd^{2+} on the adsorbents. Undabeytia et al. [44] also reported apparent hysteresis of Cd^{2+} after three cycles of desorption from montmorillonite SAz-1. Saha et al. [45] observed that large fractions of sorbed Cd^{2+} were retained by montmorillonite, hydroxyaluminum- and hydroxyaluminosilicate-montmorillonite complexes.
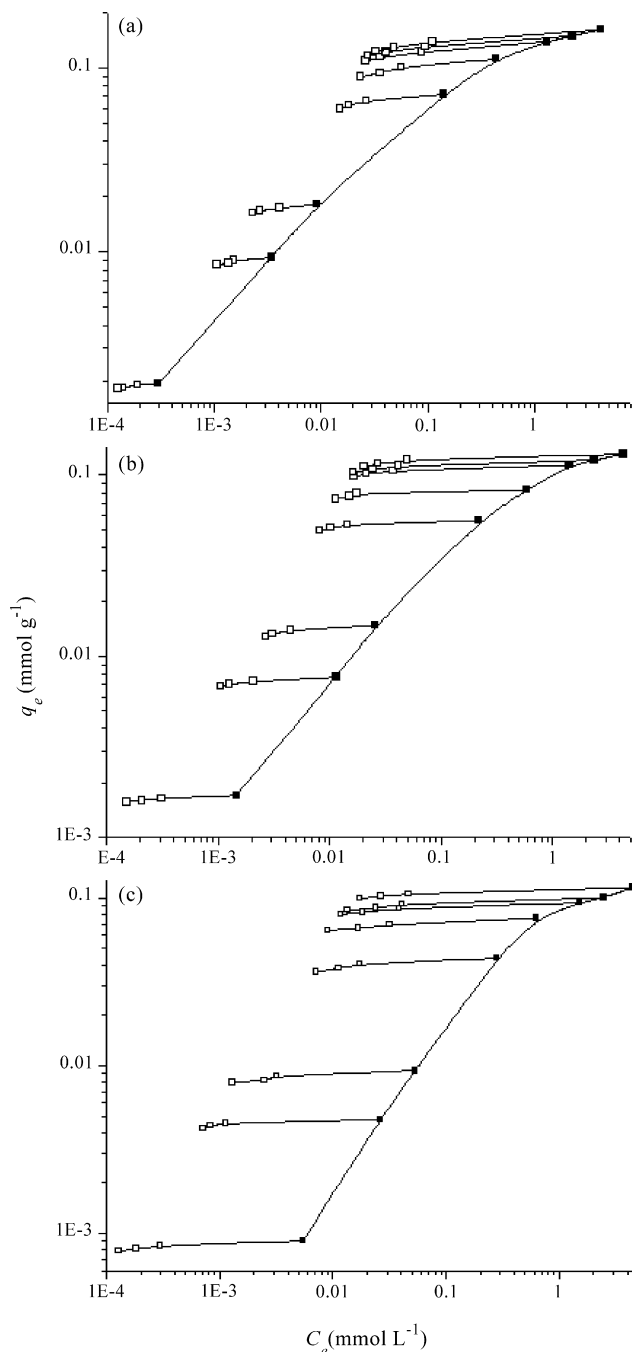

Fig. 7. Adsorption (■)–desorption (□) isotherms of Cd^{2+} on Al$_{13}$-PAAMt (a), Al$_{13}$-PMt (b) and Na$^+$-Mt (c).

The distribution coefficient (k_d) is defined as the ratio of metal adsorbed on the solid phase to the free metal remaining in the aqueous phase when the system is at equilibrium. The average distribution coefficients ($\bar{k}_d$) calculated based on desorption isotherms were always greater than those calculated from the adsorption isotherms (Table 4). This indicated that the affinity of Cd^{2+} for the montmorillonites increased from the forward (adsorption) to the reverse (desorption) direction. This increase in affinity has been defined as an indicator of hysteresis by Essington [46] and similar hysteresis has been reported for the adsorption of Cd by palygorskite, sepiolite and calcite [47].

Table 4

Average Cd^{2+} distribution coefficients $\bar{k}_d$ (L g^{-1}) obtained from adsorption and desorption data

	Initial Cd^{2+} added (mmol L^{-1})	Al_{13}-PAAMt	Al_{13}-PMt	Na^+-Mt
Adsorption	–	1.509	0.3707	0.1163
Desorption	0.01	12.35	7.767	4.470
	0.05	6.718	5.179	5.089
	0.1	5.816	4.094	4.067
	0.5	3.290	4.886	3.583
	1.0	2.745	5.344	4.387
	2.0	2.896	4.487	4.522
	3.0	2.876	4.478	4.059
	5.0	2.570	4.039	3.951

4. Conclusions

In this work, Al_{13}-PAAMts were prepared under optimized conditions and used for Cd^{2+} adsorption. Their structure and adsorption performance were evaluated. The results showed that basal spacing, specific surface area and total pore volume were increased due to the intercalation of inorganic polyoxycations after pillaring. Adsorption of Cd^{2+} on these pillared montmorillonites increased with increasing pH. Al_{13}-PAAMt had a higher affinity for Cd^{2+} than either Al_{13}-PMt or Na^+-Mt. The adsorption of Cd^{2+} displayed a clearer adsorption edge on Al_{13}-PAAMt and Al_{13}-PMt than on Na^+-Mt. The adsorption kinetics of Al_{13}-PAAMt and Al_{13}-PMt were faster than that of Na^+-Mt and a pseudo-second-order model fit the experimental data. Hysteretic desorption was observed.

Acknowledgement

References

[1] ATSDR, Agency for Toxic Substances and Disease Registry, Department of Health and Human Services, USA, 1999.

[2] S. Babel, T.A. Kurniawan, Low-cost adsorbents for heavy metals uptake from contaminated water: a review, J. Hazard. Mater. B97 (2003) 219–243.

[3] M.B. McBride, Environmental Chemistry of Soils, Oxford University Press, New York, 1994.

[4] F. Barbier, G. Duc, M. Petit-Ramel, Adsorption of lead and cadmium ions from aqueous solution to the montmorillonite: water interface, Colloids Surf. A 166 (2000) 153–159.

[5] T.J. Pinnavaia, Intercalated clay catalysts, Science 220 (1983) 365–371.

[6] P. Komadel, Chemically modified smectites, Clay Miner. 38 (2003) 127–138.

[7] K.A. Carrado, Synthetic organo- and polymer-clays: preparation, characterization, and materials applications, Appl. Clay Sci. 17 (2000) 1–23.

[8] A. Vaccari, Preparation and catalytic properties of cationic and anionic clays, Catal. Today 41 (1998) 53–71.

[9] M.J. Hernando, C. Pesquera, C. Blanco, F. González, Comparative study of the texture of montmorillonites pillared with aluminum and aluminum/cerium, Langmuir 17 (2001) 5156–5159.

[10] P. Salerno, S. Mendioroz, Preparation of Al-pillared montmorillonite from concentrated dispersions, Appl. Clay Sci. 22 (2002) 115–123.

[11] A. Aouad, T. Mandalia, F. Bergaya, A novel method of Al-pillared montmorillonite preparation for potential industrial up-scaling, Appl. Clay Sci. 28 (2005) 175–182.

[12] J.B. Harsh, H.E. Doner, Specific adsorption of copper on a hydroxy-aluminum-montmorillonite complex, Soil Sci. Soc. Am. J. 48 (1984) 1034–1039.

[13] L. Bergaoui, J.-F. Lambert, H. Suquet, M. Che, Cu^{II} on Al_{13}-Pillared saponites: macroscopic adsorption measurements and EPR spectra, J. Phys. Chem. 99 (1995) 2155–2161.

[14] L. Bergaoui, I. Mrad, J.-F. Lambert, A. Ghorbel, A comparative study of the acidity toward the aqueous phase and adsorptive properties of Al_{13}-pillared montmorillonite and Al_{13}-pillared saponite, J. Phys. Chem. B 103 (1999) 2897–2902.

[15] P. Keizer, M.G.M. Bruggenwart, Adsorption of heavy metals by clay–aluminum hydroxide complexes, in: G.H. Bolt, et al. (Eds.), Interactions at the Soil Colloid–Soil Solution Interface, Kluwer Academic Publ., Dordrecht, The Netherlands, 1991, pp. 177–203.

[16] K. Sakurai, P.M. Huang, Influence of potassium chloride on desorption of cadmium sorbed on hydroxyaluminosilicate-montmorillonite complex, Soil Sci. Plant Nutr. 42 (1996) 475–481.

[17] U.K. Saha, S. Taniguchi, K. Sakurai, Adsorption behavior of cadmium, zinc, and lead on hydroxyaluminum- and hydroxyaluminosilicate-montmorillonite complexes, Soil Sci. Soc. Am. J. 65 (2001) 694–703.

[18] B. Lothenbach, G. Furrer, R. Schulin, Immobilization of heavy metals by polynuclear aluminum and montmorillonite compounds, Environ. Sci. Technol. 31 (1997) 1452–1462.

[19] S.S. Gupta, K.G. Bhattacharyya, Removal of Cd(II) from aqueous solution by kaolinite, montmorillonite and their poly(oxo zirconium) and tetrabutylammonium derivatives, J. Hazard. Mater. 128 (2006) 247–257.

[20] H. Jobstmann, B. Singh, Cadmium sorption by hydroxyl-aluminium interlayered montmorillonite, Water Air Soil Pollut. 131 (2001) 203–215.

[21] B. Lothenbach, R. Kerbs, G. Furrer, S.K. Gupta, R. Schulin, Immobilization of cadmium and zinc in soil by Al-montmorillonite and gravel sludge, Eur. J. Soil Sci. 49 (1998) 141–148.

[22] U.K. Saha, S. Taniguchi, K. Sakurai, Simultaneous adsorption of cadmium, zinc, and lead on hydroxyaluminum- and hydroxyaluminosilicate-montmorillonite complexes, Soil Sci. Soc. Am. J. 66 (2002) 117–128.

[23] E.G. Pradas, M.V. Sánchez, F.C. Cruz, M.S. Viciana, M.F. Perez, Adsorption of cadmium and zinc from aqueous solution on natural and activated bentonite, J. Chem. Technol. Biotechnol. 59 (1994) 289–295.

[24] G. Suraj, C.S.P. Iyer, M. Lalithambika, Adsorption of cadmium and copper by modified kaolinites, Appl. Clay Sci. 13 (1998) 293–306.

[25] T. Vengris, R. Binkienē, A. Sveikauskaitē, Nickel, copper and zinc removal from waste water by a modified clay sorbent, Appl. Clay Sci. 18 (2001) 183–190.

[26] K.G. Bhattacharyya, S.S. Gupta, Pb(II) uptake by kaolinite and montmorillonite in aqueous medium: Influence of acid activation of the clays, Colloids Surf. A 227 (2006) 191–200.

[27] R. Mokaya, W. Jones, Pillared acid-activated clay catalysts, J. Chem. Soc., Chem. Commun. 8 (1994) 929–930.

[28] R. Mokaya, W. Jones, Pillared clays and pillared acid-activated clays: a comparative study of physical, acidic, and catalytic properties, J. Catal. 153 (1995) 76–85.

[29] R. Mokaya, W. Jones, The microstructure of alumina pillared acid-activated clays, J. Porous Mat. 1 (1995) 97–110.

[30] R. Mokaya, W. Jones, M.E. Davies, M.E. Whittle, Preparation of alumina-pillared acid-activated clays and their use as chlorophyll adsorbents, J. Mater. Chem. 3 (1993) 381–387.

[31] J. Bovey, W. Jones, Characterisation of Al-pillared acid activated clay catalysts, J. Mater. Chem. 5 (1995) 2027–2035.

[32] F. Qin, X. Shan, B. Wei, Effects of low-molecular-weight organic acids and residence time on desorption of Cu, Cd, and Pb from soils, Chemosphere 57 (2004) 253–263.

[33] O. Abollino, M. Aceto, M. Malandrino, C. Sarzanini, E. Mentasti, Adsorption of heavy metals on Na-montmorillonite. Effect of pH and organic substances, Water Res. 37 (2003) 1619–1627.

[34] Y.-S. Ho, Review of second-order models for adsorption systems, J. Hazard. Mater. 136 (2006) 681–689.

[35] A. Bentouami, M.S. Ouali, Cadmium removal from aqueous solutions by hydroxy-8 quinoleine intercalated bentonite, J. Colloid Interface Sci. 293 (2006) 270–277.

[36] W.J. Weber, J.C. Morris, Kinetics of adsorption on carbon from solution, J. Sanit. Eng. Div. Am. Soc. Civ. Eng. 89 (1963) 31–60.

[37] N.K. Lazaridis, D.D. Asoohidou, Kinetics of sorptive removal of chromium (VI) from aqueous solutions by calcined Mg–Al–CO$_3$ hydrotalcite, Water Res. 37 (2003) 2875–2882.

[38] D.M. Manohar, B.F. Noeline, T.S. Anirudhan, Adsorption performance of Al-pillared bentonite clay for the removal of cobalt(II) from aqueous phase, Appl. Clay Sci. 31 (2006) 194–206.

[39] X.-S. Wang, J. Huang, H.-Q. Hu, J. Wang, Y. Qin, Determination of kinetic and equilibrium parameters of the batch adsorption of Ni(II) from aqueous solutions by Na-mordenite, J. Hazard. Mater. 142 (2007) 468–476.

[40] P. Janoš, J. Sypecká, P. Mlčkovská, P. Kuráň, V. Pilařoá, Removal of metal ions from aqueous solutions by sorption onto untreated low-rank coal (oxihumolite), Sep. Purif. Technol. 53 (2007) 322–329.

[41] W. Matthes, F.T. Madsen, G. Kahr, Sorption of heavy-metal cations by Al and Zr-hydroxy-intercalated and pillared bentonite, Clays Clay Miner. 47 (1999) 617–629.

[42] C.W. Cheung, C.K. Chan, J.F. Porter, G. McKay, Film-pore diffusion control for the batch sorption of cadmium ions from effluent onto bone char, J. Colloid Interface Sci. 234 (2001) 328–336.

[43] M. Machida, Y. Kikuchi, M. Aikawa, H. Tatsumoto, Kinetics of adsorption and desorption of Pb (II) in aqueous solution on activated carbon by two-site adsorption model, Colloids Surf. A 240 (2004) 179–186.

[44] T. Undabeytia, S. Nir, G. Rytwo, E. Morillo, C. Maqueda, Modeling adsorption–desorption processes of Cd on montmorillonite, Clays Clay Miner. 46 (1998) 423–428.

[45] U.K. Saha, K. Iwasaki, K. Sakurai, Desorption behavior of Cd, Zn and Pb on hydroxyaluminum- and hydroxyaluminosilicate-montmorillonite complexes, Clays Clay Miner. 51 (2003) 481–492.

[46] M.E. Essington, Soil and Water Chemistry: An Integrative Approach, CRC Press, Boca Raton, Florida, 2004.

[47] M. Shirvani, M. Kalbasi, H. Shariatmadari, F. Nourbakhsh, B. Najafi, Sorption–desorption of cadmium in aqueous palygorskite, sepiolite, and calcite suspensions: isotherm hysteresis, Chemosphere 65 (2006) 2178–2184.